

Analysis of wxAmps Results for a New Dye Sensitized Solar Cell using Solid State Electrolyte and Graphene

Mahsa Narimani¹ Karim Abbasian², and Gholamreza Kiani³

¹ Master of Science- Nanotechnology Engineering, Aras International campus, University of Tabriz, Tabriz, 5166614761, Iran

^{2,3} Associate Professor, School of Engineering-Emerging Technologies, University of Tabriz, Tabriz 5166614761, Iran

Abstract

A dye-sensitized solar cell (DSSC) with a nanocrystalline TiO₂ film electrode on ITO glass, N719 dye, CsSnI₃ as solid state electrolyte to solve constancy problems such as electrode corrosion and electrolyte permeation, and counter WO₃ electrode, designed and simulated by wxAmps software. As research results has proved, that select graphene as 2D bridges into the nanocrystalline electrodes of dye-sensitized solar cells, which brought a faster electron transport and a lower recombination, together with a higher light scattering³. Compared to 1D nanomaterials and liquid electrolytes using in typical DSSCs, this simulation's results show more excellent properties and energy conversion efficiency (20.7102%).

Keywords:

Dye-sensitized Solar Cells, Graphene, TiO₂, CsSnI₃, Simulation

1. Introduction

Since 1991, dye-sensitized solar cells (DSSCs) have been improved due to their low fabrication cost and relatively high conversion efficiency. Light-to-electron conversion efficiency of DSSCs was achieved over 10%, which is still short of silicon's performance. DSSCs usually consist of a high porosity of nanocrystalline photoanode made of TiO₂ semiconductor deposited on a transparent conducting oxide (TCO) or Indium tin oxide (ITO) glass support and sensitized with a self-assembled monolayer of dye molecules anchored to the TiO₂ surface. When illuminated, the dye molecules capture the incident photons generating electron-hole pairs. The resultant electrons are immediately injected into the conduction band of the TiO₂ and transported to the electron-collecting counter electrode. Regeneration of dye molecules is accomplished by capturing electrons usually from a liquid electrolyte (iodide/iodine solution)¹. Typical dye-sensitized solar cells suffer from durability problems that result from their use of organic liquid electrolytes containing the iodide/tri-iodide redox couple, which causes serious problems such as electrode corrosion and electrolyte leakage. Replacements for iodine-based liquid electrolytes have been extensively studied, but the efficiencies of the resulting devices remain low. According to research results² that show the solution-

processable p-type direct bandgap semiconductor CsSnI₃ can be used for hole conduction in lieu of a liquid electrolyte. Moreover; in DSSCs; the major bottleneck is the transport of photogenerated electrons across the TiO₂ nanoparticle network, which competes with the charge recombination. To suppress the recombination and improve the transport, one of strategies is including; introducing charge carriers (1D nanomaterials like carbon nanotubes) to direct photogenerated electron. However, the efficiency was increased limitedly because of the point contact between nanosphere TiO₂ and columniform 1D nanomaterials. In the photovoltaic area, graphene is a promising material improving the performance of solar cells. It is a zero band gap material and electrons in it are just like massless relativistic particles, so it has an excellent electrical conduction in two dimensions even at temperatures close. Herein, we designe and simulat a new DSSC to solve the most usual problems in these types, by simultaneous using of graphene and CsSnI₃ in one cell. As research results tell us; graphene bridges can enhance the charge transport rate to prevent the charge recombination and increase the light collection efficiency. On the other side, CsSnI₃, because of its energy gap (1.3 eV) and a remarkably high hole mobility of $\mu_h=585 \text{ cm}^2\text{V}^{-1} \text{ s}^{-1}$ at room temperature, is well fitted

Characterization of CsSnI₃ in DSSCs: CsSnI₃ replaces the entire liquid electrolyte. Optical absorption spectroscopy and incident photon-to-current conversion efficiency (IPCE) measurements show that our cells exhibit a red shifted absorption edge (at 789 nm) compared to that of the typical Grätzel cell and outperform it in the red and infrared spectral regions. The key characteristics of CsSnI₃ in DSSC is that (1) it is solution-processable, and thus permeates throughout the entire TiO₂ structure, allowing facile charge separation and hole removal, and (2) it

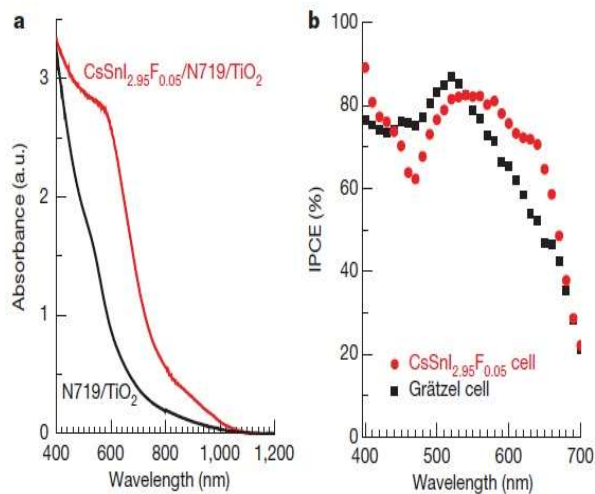


Figure 1 Optical response of the $\text{CsSnI}_{2.95}\text{F}_{0.05}$ cell and a conventional Grätzel cell. a, Optical absorbance spectra of the devices consisting of $\text{CsSnI}_{2.95}\text{F}_{0.05}$ /N719 dye/ TiO_2 (red line) and N719 dye/ TiO_2 (liquid electrolyte was not added here) (black line). b, The IPCE spectrum as a function of the wavelength of monochromatic light that impinges on the $\text{CsSnI}_{2.95}\text{F}_{0.05}$ cell (filled circles) in comparison with that of the N719-dye-containing Grätzel cell (filled squares).²

The optical absorption spectrum of the $\text{CsSnI}_{2.95}\text{F}_{0.05}$ -containing cell, obtained in transmission mode, reveals a well-defined edge at 789 nm, which is significantly red-shifted from that of the Grätzel cell with N719 dye, at 667nm (Figure. 1a). This observation indicates that the cell absorbs red and near-infrared light more efficiently than the Grätzel cell. Note that lack of sunlight absorption in the red and near-infrared regions has been a challenge for typical ruthenium-based dyes. Figure 1b compares the incident photon-to-current conversion efficiency (IPCE) as a function of excitation wavelength for the $\text{CsSnI}_{2.95}\text{F}_{0.05}$ cell with the Grätzel cell. The IPCE spectrum is a measure of the light response of photovoltaic devices, which is directly related to the short-circuit current. In the 550-670nm spectral range, this cell produces a higher and broader photocurrent density in the external circuit under monochromatic illumination (per photon flux). Note that the upper limit of our IPCE measurement setting is 700 nm, resulting in a sharp drop beyond 670nm.

2. Graphene-containing Cells

Graphene is a 2D soft single molecular layered structure, and there are intermolecular forces such as physisorption, electrostatic binding, or charge transfer interactions between graphene and TiO_2 so the nanocrystalline TiO_2 can anchor on the graphene flake compactly (Figure 2b) to form

graphene bridges, which will decrease the TiO_2 - TiO_2 contacts. The graphene bridged enhance the electron transport from the conduction band (CB) of TiO_2 at the anchor position quickly (Figure 2d), and the recombination is reduced as a result.

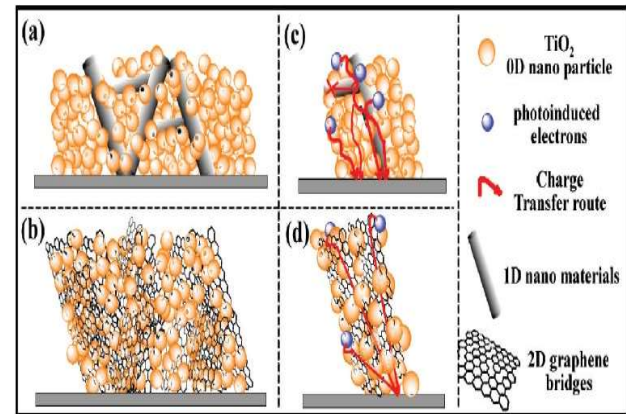


Figure 2 Differences between (a,c) 1D and (b,d) 2D nanomaterial composite electrodes. In 2D nanomaterial composite electrodes (graphene bridges), the TiO_2 particles can anchor in the graphene better, and the photoinduced electrons can be captured and transferred by the graphene; however, with the 1D nanomaterial compositing, there are less intermolecular forces and connection between TiO_2 and the 1D nanomaterial; therefore, the transfer barrier is larger and the recombination is much easier to happen.

Due to its excellent electrical conduction, the 2D graphene bridges behave as an electron transfer channel, which can transport the photoinduced electron quickly, and the energy level of graphene is between the CB of TiO_2 and ITO. Under illumination, the CB of semiconductor TiO_2 receives the electrons from photoexcited dye. Because the TiO_2 is anchored with 2D graphene, and the graphene is homogeneous in the system, the excited electrons are captured by the graphene without any obstruction. The collected electrons can transport from TiO_2 to the conductive substrate quickly and effectively through graphene bridges (Figure 2d), and hence the adverse reactions (recombination and back reaction) are suppressed.

wxAMPS program: The computer models can be used as a method that leads to a better device design. Device modelling involves the numerical solution of a set of equations, which form a mathematical model for device operation. The usefulness of the simulation results strongly depends on the reliability of the input parameters that are required by the internal numerical models. By using simulation programs it is possible to examine the influence of model parameters, which cannot be determined experimentally. The one-dimensional device simulation

program AMPS solves Poisson equation and the electron and hole continuity equations by using the method of finite differences and the Newton-Raphson technique (Pennsylvania State University, 1997)⁴. wxAMPS program was developed at the University of Illinois Urbana Champagne in collaboration with NANKAI University of China, which uses the physical rules of the AMPS program. In this program, tunneling characteristics are added to the simulation process and simulation homology characteristics improved. Compare to AMPS program; the outputs of wxAMPS have been improved and are more accurately displayed. Some of the outputs of this software are: 1- current - Voltage, 2-Energy band, 4- Current Density, 5- Quantum efficiency

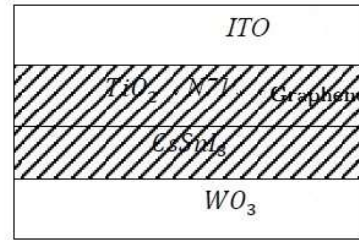


Figure 3. Structure of a dye sensitized solar cell using solid state electrolyte and graphene

The incident photon is under AM1.5 conditions and temperature equal 298.15k or 25°. Table 1 shows the electrical parameters of active layer of structure.

3. Results and Discussion

This part shows the simulation results of all solid-state, inorganic solar cell system structure that consists of the p-type direct bandgap semiconductor CsSnI₃ and n-type nanoporous TiO₂ with graphene bridges and the dye N719 (cisdiisothiocyanato-bis(2,29-bipyridyl-4,4'-dicboxylato) ruthenium(II) bis-(tetrabutylammonium)). Scheme 1 show a simple structure of our study. The thickness of active layer is about 1300 nm.

Table 2 Electrical parameters of active layer

Input parameters for the numerical: N_c and N_v are the band effective densities of states for the conduction and valence bands, N_d and N_a are donor and acceptor concentration, U_n and U_p are recombination rate for electrons and holes; respectively

Layer	TiO ₂	CcSnI ₃
Thickness (mm)	100	1200
Permittivity	100	60
E _g (eV)	3.2	1.2
Affinity (eV)	4.26	3.62
N_c (cm ⁻³)	10 ²¹	10 ¹⁷
N_v (cm ⁻³)	6.9×10 ¹⁹	10 ¹⁷
U_n (cm ² /V/s)	10 ⁻¹	15000
U_p (cm ² /V/s)	2×10 ⁻³	15000
N_d (cm ⁻³)	0	0
N_a (cm ⁻³)	5×10 ¹⁰	5×10 ²⁰

Three of the semiconductor device equations (the Poisson equation and the electron and hole continuity equations) are solved by wxAMPS, and we need to apply the parameters of the utilized materials to the program. Used physical constants are listed in Table 1 and the capture, recombination and generation times are estimated as physical parameters in the model.

Current -Voltage (I-V) curves: one of the most important solar cell curves is the (I-V) curve. The obtained I-V curve of the cell is shown in Figure 3.

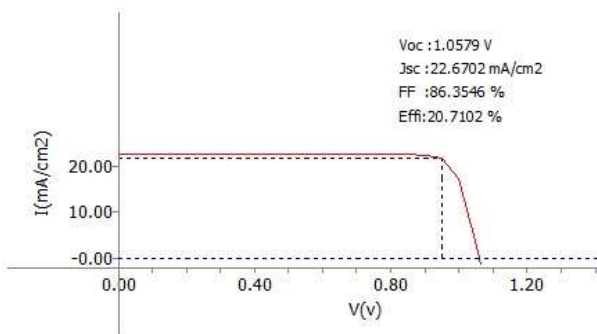


Figure. 3 Current-voltage curves under illumination

Three of the most important dye-sensitized solar cell output parameters are: 1- open-circuit voltage (V_{oc}), 2- short-circuit current density (J_{sc}), 3- fill factor (FF). The last parameter an output (E_{ffi}), shows the efficiency of solar cells. The achieved results are the energy conversion efficiency %20.7102 ($V_{oc}=1.0579V$, $J_{sc}=22.6702$ mA/cm², $FF=0.8635$).

When the solar cell is operated under a condition that gives the maximum output power, the voltage V_m and the current I_m at the optimal operation point is shown in Figure 3. The fill factor FF of the solar cell is defined as

$$FF = \frac{V_m I_m}{V_{oc} I_{sc}} \quad (1)$$

The FF in expression (1), has a typical value between zero and one. According to the Figure 3, the current - voltage curve is close to rectangular shape. The amount proximity curve rectangular shape with a quantity called the fill factor (FF) is expressed. That whatever amount this is closer to the number one, the solar cell will be of high quality.

Energy Bands Curve: Semiconductors that we have used in solar cells are different in band gap and thickness, as shown in Figure 3. Black lines show the band edge of the semiconductors. Which black lines on the top conduction

band (E_c), black line on the bottom the valence band (E_v), the blue line is the quasi-Fermi- level of electrons (E_{fn}) and the red line is the quasi-Fermi- level of holes (E_{fp}) shows. Due to the band gap semiconductors are different from each. In the moment of connecting with each other semiconductor depletion region comes into existence, as you can see in Figure 4.

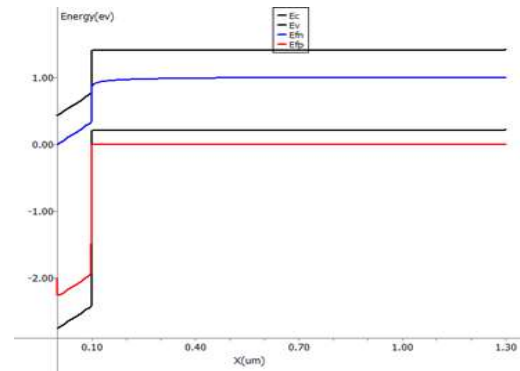


Figure 4 Energy Band gap curves

Current Density Curves: The electric current density is a function of the amount of current passing through the surface point and perpendicular to the direction of flow is measured. The quantity briefly with J show⁵, as you can see in Figure 5. The carriers current density compared to the thickness of the semiconductor shows. The blue line is the electron current density, red line the hole current density and black line indicates the total current density. Then given that the semiconductor, electrons and holes in the covers. The total current density is the sum of the electrons.

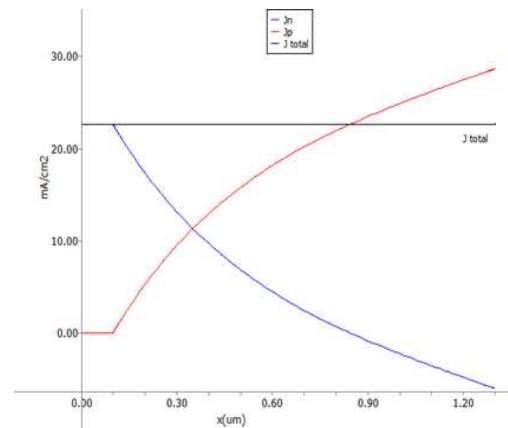


Figure 5 Current density curves

Quantum Efficiency (QE) Curves: The " quantum efficiency " (Q.E.) is the ratio of the number of carriers collected by the solar cell to the number of photons of a given energy incident on the solar cell. The quantum efficiency may be given either as a function of wavelength

or as energy. If all photons of certain wavelength are absorbed and the resulting minority carriers are collected, then the quantum efficiency at that particular wavelength is unity. The quantum efficiency for photons with energy below the band gap is zero. A quantum efficiency curve for a dye sensitized solar cell is shown below. QE = 100% means that one incident photon can generate one electron Figure 6 shows quantum efficiency curves. The amount of current generated by incident photons of a particular wavelength is, as you see in Figure 6. Quantum efficiency curves have been divided into several sections. Section 1, which shows the quantum efficiency of dye-sensitized solar cell. Section 2 is reduced quantum efficiency. Section 3 is reduced quantum efficiency. The main reason is that recombination has occurred in the back of the dye-sensitized solar cells. Section 4, the reflection losses.

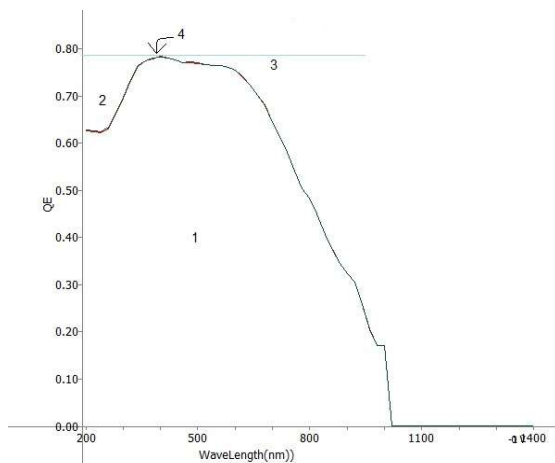


Figure 6 Quantum efficiency (QE) curves

4. Conclusion

In summary, 2D graphene is a rising star in material science, and we use of its high mobility in our simulation of DSSC successfully. The short-circuit current density increased to 22.6702 mA/cm², this may be due to a lower recombination and a faster electron transport with the introduction of graphene chiefly. The past studies use graphene bridges in a DSSC with liquid electrolyte or use solid state electrolyte without improving the speed of electron transport or other ways, but we designed and simulated a DSSC; without the past leakage or problems without the past leakage or problems and that reaches.

References

- [1]. Sanghun Lee, Hyunjune Park, Taehee Park, Jongtaek Lee, and Whikun Yi, "Some Features of Dye-sensitized Solar Cell Combining with Single-walled Carbon Nanotubes"
- [2]. In Chung, Byunghong Lee, Jiaqing He, Robert P. H. Chang, Mercouri G. Kanatzidis, "All-solid-state dye-sensitized solar cells with high efficiency "
- [3]. N. Yang, J. Zhai, D. Wang, Y. Chen, L. Jiang, " Two-Dimensional Graphene Bridges Enhanced Photoinduced Charge Transport in Dye-Sensitized Solar Cells "
- [4]. Samah G. Babiker, Yong Shuai, " Simulation of Organic Solar Cells Using AMPS-1D Program "
- [5] Soga, T., (editor), " Nanostructured Materials for Solar Energy Conversion" (Fundamentals of Solar Cell), Elsevier, (2006).
- [6]. Liu, Yiming, Yun Sun, and Angus Rockett. "A new simulation software of solar cells—wxAMPS." *Solar Energy Materials and Solar Cells* 98 (2012): 124-128.
- [7]. Koh, J. K., Kim, J., Kim, B., Kim, J. H. & Kim, E. Highly efficient, iodine-free dyesensitized solar cells with solid-state synthesis of conducting polymers.
- [8]. Yanagida, S., Yu, Y. H. & Manseki, K. Iodine/iodide-free dye- sensitized solar cells. *Acc. Chem. Res.* 42, 1827- 1838 (2009).
- [9]. Lee, B., Buchholz, D. B., Guo, P. J., Hwang, D. K. & Chang, R. P. H. Optimizing the performance of a plastic dye-sensitized solar cell. *J. Phys. Chem. C* 115, 9787–9796 (2011).
- [10]. Lee, B. et al. Materials, interfaces, and photon confinement in dye-sensitized solar cells. *J. Phys. Chem. B* 114, 14582–14591 (2010).
- [11]. Sefunc, M. A., A. K. Okyay, and H. V. Demir. (2011) . "Plasmonic backcontact grating for P3HT:PCBM organic solar cells enabling strong optical absorption increased in all polarizations." *Optics Express* 19(15): 14200-14209.
- [12]. Xi, Junting, et al. " Growth of single-crystalline rutile TiO₂ nanorods on fluorine-doped tin oxide glass for organic-inorganic hybrid solarcells." *Journal of Materials Science: Materials in Electronics* 23.9 (2012): 1657-1663.
- [13]. Liu, Yiming, Yun Sun , and Angus Rockett. " Batch simulation of solar cells by using Matlab and wxAMPS." *Photovoltaic Specialists (PVSC), 2012 38 th IEEE. IEEE,2012.*
- [14]. Mandoc, M. M., L. J. A. Koster, and P. W. M. Blom. " Optimum charge carrier mobility in organic solar cells." *Applied physics letters* 90.13 (2007): 133504-133504.